HHS Public Access

Author manuscript

Radiother Oncol. Author manuscript; available in PMC 2017 February 01.

Published in final edited form as:

Radiother Oncol. 2016 February ; 118(2): 315–322. doi:10.1016/j.radonc.2016.01.011.

Magnetic Resonance Imaging of Swallowing-Related Structures in Nasopharyngeal Carcinoma Patients Receiving IMRT: Longitudinal Dose-Response Characterization of Quantitative Signal Kinetics

Jay A. Messer, BS[1,5,*], **Abdallah S. R. Mohamed, MD, M.Sc.**[1,6,*], **Katherine A. Hutcheson, PhD**[2], **Yao Ding, PhD**[3], **Jan S. Lewin, PhD**[2], **Jihong Wang, PhD**[3], **Stephen Y. Lai, MD, PhD**[2], **Steven J. Frank, MD**[1], **Adam S. Garden, MD**[1], **Vlad Sandulache, MD**[2], **Hillary Eichelberger, BA, BS**[1,5], **Chloe C. French, BS**[1,5], **Rivka R. Colen, MD**[4], **Jack Phan, MD, PhD**[1], **Jayashree Kalpathy-Cramer, PhD**[7], **John D. Hazle, PhD**[3], **David I. Rosenthal, MD**[1], **G. Brandon Gunn, MD**[1], and **Clifton D. Fuller, MD, PhD**[1,*]

[1]Department of Radiation Oncology, The University of Texas MD Anderson Cancer Center, Houston, TX, USA

[2]Department of Head and Neck Surgery, The University of Texas MD Anderson Cancer Center, Houston, TX, USA

[3]Department of Imaging Physics, The University of Texas MD Anderson Cancer Center, Houston, TX, USA

[4]Department of Diagnostic Imaging, The University of Texas MD Anderson Cancer Center, Houston, TX, USA

[5]The University of Texas Medical School at Houston, TX, USA

[6]Department of Clinical Oncology and Nuclear Medicine, Faculty of Medicine, University of Alexandria, Alexandria, Egypt

[7]Department of Radiology, Harvard Medical School, Boston, MA, USA

Abstract

Background—We aim to characterize serial (i.e., acute and late) MRI signal intensity (SI) changes in dysphagia-associated structures as a function of radiotherapy (RT) in nasopharyngeal cancer (NPC) patients.

Materials and Methods—We retrospectively extracted data on 72 patients with stage III-IV NPC treated with intensity-modulated RT (IMRT). The mean T1- and T2-weighted MRI SIs were

[*]Corresponding authors: Clifton D. Fuller, MD, PhD: Head and Neck Section, Division of Radiation Oncology, Department of Radiation Oncology, The University of Texas MD Anderson Cancer Center, 1515 Holcombe Blvd, Unit 97, Houston, TX 77030. Tel: (713) 563-2334 cdfuller@mdanderson.org, Abdallah S. R. Mohamed, MD, MSc: Head and Neck Section, Division of Radiation Oncology, Department of Radiation Oncology, The University of Texas MD Anderson Cancer Center, 1515 Holcombe Blvd, Unit 97, Houston, TX 77030. Tel: (832) 955-7920 asmohamed@mdanderson.org, Jay A. Messer, BS: Head and Neck Section, Division of Radiation Oncology, Department of Radiation Oncology, The University of Texas MD Anderson Cancer Center, 1515 Holcombe Blvd, Unit 97, Houston, TX 77030. Tel: (512) 565-6071 Jay.A.Messer@uth.tmc.edu.

recorded for the superior pharyngeal constrictor (SPC) and soft palate (SP) at baseline, early-after IMRT, and last follow up, with normalization to structures receiving <5 Gy.

Results—All structures had a significant increase in T2 SIs early after treatment, irrespective of the mean dose given. At last follow-up, the increase in T2 SI subsided completely for SPC and partially for SP. The T1 SI did not change significantly in early follow-up images of both structures; on late follow-up, patients with mean doses >62.25 Gy had significant decrease in the corresponding T1 SI for SPC (1.6 ± 0.4 vs. 1.3 ± 0.4, P=0.007) but decreased non-significantly for SP.

Conclusions—Serial MRI acquisitions enable the identification of both early and late radiation-induced changes in swallowing structures after definitive IMRT for NPC. Dose dependent decreased signal intensity on late T1 images is associated with higher RT doses to the superior pharyngeal constrictor muscle; while dose independent increased SI for both structures on early post-RT T2 images is observed and subsides after therapy. Further efforts will seek to elucidate the relationship between dose-dependent muscle SI changes and the potential functional alteration of swallowing muscles.

Keywords

Nasopharyngeal Carcinoma; Magnetic Resonance Imaging; Dysphagia; Dose-response; Superior Pharyngeal Constrictor; IMRT

Introduction

Radiation therapy (RT) for head and neck cancer can result in changes to the muscles responsible for swallowing, leading to short-term or long-term dysphagia. [1–4] In general, the early acute toxicities that are largely attributable to acute mucosal injury from RT are self-limited, whereas “late effects” occurring >90 days after therapy typically reflect progressive and irreversible fibrosis and soft tissue injury. [5–7] Since concurrent chemotherapy and RT represents the standard of care for nasopharyngeal cancer (NPC) [8, 9], chronic dysphagia can have a substantial negative impact on the quality of life of long-term survivors [7, 10–14]. Therefore, investigation into the pathophysiology and predictors of permanent dysfunction is paramount. [15]

The major muscular structures involved in the propulsive phase of swallowing are the superior pharyngeal constrictor (SPC), the middle pharyngeal constrictor, the inferior pharyngeal constrictor, the base of the tongue, the soft palate (SP), and the esophageal inlet. [16–18] Suprahyoid and floor of mouth musculature are critical for protecting the airway by preventing aspiration and penetration since they elevate the hyoid and larynx to allow for appropriate bolus diversion away from the airway and help to open the esophagus for bolus entry. [19] Many studies have reported strong correlations between dysphagia and the radiation dose to the pharyngeal constrictors. More specifically, the superior pharyngeal constrictor dose has been identified as a strong correlate and predictor of long-term, dose-related, radiation-associated dysphagia (RAD). [15, 20] During deglutition, the soft palate functions to both prevent premature entry of the bolus into the unprepared pharynx and to provide a velopharyngeal seal to allow distal driving pressure during pharyngeal transit. [18]

While the effects of RAD on the soft palate have not been studied as extensively as those on the superior pharyngeal constrictor, it typically receives a large dose of radiation in the treatment of NPC and is a logical organ-at-risk to study.

For several years, magnetic resonance imaging (MRI) has been used to track radiation-induced changes in normal tissue. [21, 22] Irradiation of the pharyngeal wall results in T2-weighted signal intensity (SI) increases and T1-weighted SI decreases, reflecting radiation-induced edema and fibrosis, respectively. The T2-weighted sequence is sensitive at detecting even slight mucosal edema, represented by high SI. [23] Consequently, the use of such techniques could provide a method of assessing post-therapy injury, potentially even before the clinically apparent development of late RT sequelae. [24]

Other investigators have studied MRI SI changes that occur after head and neck RT and the qualitative pathophysiological characteristics of these changes [21–23], and preliminary data indicative of dose-dependent changes have been identified in a general head and neck dataset; however, to our knowledge, no study has tracked serial (i.e., acute and late) quantitative dose-response MRI parameter kinetics in a uniform NPC dataset.

The aim of this retrospective study is to characterize serial MRI SI changes that are indicative of RT-induced changes in dysphagia-associated volumes of interest (VOIs) as a function of the radiation dose. Our investigation serves as a hypothesis-generating study for a prospective clinical trial set to validate the T1 and T2 SI changes in correlation with patient treatment toxicity data.

Materials and Methods

Patients

The study was approved by the institutional review board of The University of Texas MD Anderson Cancer Center (Houston, Texas). Data were extracted from electronic medical records for all patients with stage III-IV NPC who had been treated with curative intensity-modulated RT (IMRT) between 2002 and 2013 as part of a programmatic investigation into therapeutic outcomes for NPC. [25] The criteria included a proven pathologic diagnosis of NPC, treatment with curative intent, no prior RT to the head and neck area, available baseline pretreatment MRI, no evidence of recurrence or salvage therapy, and 2 or more serial MRIs after therapy.

MRI

For each patient, serial T1- and T2-weighted diagnostic MRIs had been obtained at baseline (pre-IMRT), early after IMRT, and at last follow-up after IMRT (Figure 1 a–c). The head and neck MRI images were obtained using a 1.5T Signa Excite MRI scanner (GE Healthcare, Waukesha, WI) with T1-weighted images (spin echo (SE), TE 8–24 ms, TR 50–800 ms, slice thickness 3–5 mm, matrix 256×256 without fat suppression) and T2-weighted images (fast spin echo (FSE), TE 69–108 ms, TR 3000–6500 ms, slice thickness 3–5 mm, echo train length 16, matrix 256×256with fat suppression) and patients lying in the supine position. The effect of TR and TE variation on signal intensity changes is described in details in the supplementary online data.

Image segmentation and registration

The mean T1- and T2-weighted MRI signal intensities (SIs) were recorded at each time point for the segmented VOIs, including the superior pharyngeal constrictor and the soft palate. While there are many candidate dysphagia structures of interest, we chose these structures as they are routinely imaged as part of skull base protocols. Using axial MRI slices for both VOIs, we contoured the superior pharyngeal constrictor from the level of the caudal pterygoid plates to the upper border of the hyoid bone; the soft palate was contoured from the inferior nasal cavity to the tip of the uvula. The manually segmented superior pharyngeal constrictor and soft palate structures were propagated from baseline to subsequent follow-up images using the deformable image registration platform of a benchmarked commercial image registration software (Velocity AI, version 3.0.1, Atlanta, GA).[26, 27] Additional quality assurance review of the propagated contours was done by two expert radiation oncologists (ASRM, CDF) with manual corrections when deemed necessary. The MRI SIs of the VOIs were normalized, in the manner of Popovtzer et al [22], to structures receiving a <5 Gy cumulative dose to account for MRI variability since a negligible radiation dose to these reference regions would be expected to have a minimal effect on SIs. The T1-weighted VOIs were normalized to the ocular globe, and the T2-weighted VOIs were normalized to the caudate nucleus because these structures received no detectable radiation dose and were easily segmented in each scan. The IMRT plans were restored. Serial T1- and T2-weighted MRIs were co-registered using Velocity software with the treatment planning computed tomography images and the radiation dose grid to determine the dose-response relationship for all VOIs (Figure 1 d, e).

Statistical analysis

Time-interval-dependent T1- and T2-muscle signal alteration—A non-parametric Wilcoxon rank test statistical analysis was used, with a non-Bonferroni-corrected α=0.05 as a pre-specification for statistical significance, to compare changes in both T1 and T2 SI alteration over time, normalized to the pre-therapy baseline images. To evaluate alteration trends, we used linear regression to detect proportional alterations in T1 and T2 SI at discrete time intervals: “early” (within 12 months of therapy completion) and “late” (>12 months after RT).

Dichotomous dose-response characterization—A recursive partitioning analysis (RPA) was used to identify dichotomous dose threshold parameters associated with subsequent significant T1 and T2 SI changes, using a previously described method [28], with extracted dose-volume histogram (DVH) data in 1-cGy bins. RPA was selected over other model-dependent methods as it is ideal for discriminating “thresholds” for continuous variables when *a priori* data are scant regarding optimum “cutpoint” or “threshold” candidates; it is also statistically powerful, even in the presence of multi-collinearity or interactions within and between candidate covariates. RPA is well known in other disciplines as “Classification and Regression Trees”, developed initially by Leo Breiman as an alternative to neural networks[29]. While RPA well-known in the radiation oncology literature[30] for discriminating between categorical variables (i.e. “classification trees”), RPA can also be used with continuous discriminant variables (i.e. regression tree analysis) [31, 32]. In this case, normalized continuous change in from baseline in T1- or T2-signal

intensity was used as discriminant variable, so that we could define what dose-volume "cutpoint(s)" were associated late with a non-linear increase in T1- or T2-signal alteration.

DVH data were converted to a range of continuous doses that represented the mean dose (D_{mean}) to a VOI. Initially, RPA was performed using D_{mean} for all patients as candidates, using the normalized change from the baseline status as a discriminant variable. For decision tree partitioning, a 20% training "holdback" and a minimum split size of 10% per split/partition (i.e., 7 patients per bin) were pre-specified. An *a priori* α =0.05 was specified for significance, with iterative trees and splits accepted using a Bonferroni-corrected logworth (i.e., the natural log of the inverse p-value); subsequent pruning after the first split demonstrated non-significance to account for multiple comparisons, with 10-fold cross-validation. [28]

Post hoc confirmation of splits was performed using a confirmatory bivariate Wilcoxon comparison between trees, and the receiver-operator curve (ROC) was determined after the completion of all partitions, using derived "cutpoints" as an identified discriminator, again with a randomly selected 20% holdback verification.

Continuous (non-linear) dose-response modeling—To evaluate potential continuous dose-to-SI changes, we used the same RPA method, specifying VOI D_{mean} as a continuous discriminator variable, and normalized early and late delta mean T1 and T2 SIs as continuous candidates, with identical constraints (*vide supra*). After *post hoc* MRI SI "cutpoint" confirmation, a logistic regression analysis was performed, with the maximum likelihood fitting of probability of SI alteration assessed using 5-Gy "bins".

To characterize continuous dose responses with greater statistical robustness, we performed bootstrap resampling. A bootstrap estimation [33] of the incidence of T1 SI alteration was then performed across 1-Gy bins using 10^4 iterative replicates. Using the method of Wedenberg [34], we performed 10^4 serial curve fittings on the subsequent distributions, which provided a probabilistic estimate of the "true" population probability range of T1 SI alteration across continuous doses.

Statistical analyses were performed using JMP 11.2 Pro (SAS Institute, Cary, NC), SPSS V22 (IBM, Chicago, IL, USA), and MATLAB R2013b (MathWorks, Natick, MA, USA) statistical analytic software packages.

Results

Seventy-seven patients were extracted but only 72 patients had dose response grids recovered and therefore only these were completely analyzed. For the 72 patients, the demographic characteristics, tumor stage and grade, and RT and chemotherapy regimens are outlined in Table 1. The patients' median age at the completion of RT was 52 years, with a range between 20 and 77 years. Most of the patients were Caucasian (63%) and males (79%) and received induction chemotherapy (68%). Gross tumor (with margin) was prescribed a dose of 70 Gy in 33 fractions, and all were treated with IMRT.

The median time to early post-RT follow-up for the 72 patients was 4 months, and the median late post-RT follow-up was 41 months. The mean dose to the superior pharyngeal constrictor was 62.4 Gy (SD, 8.7 Gy), and the mean dose to the soft palate was 66.8 Gy (SD, 7.3 Gy).

Figure 2 shows 2 examples of MRI subtraction images that were created to visually depict the SI alterations between different time points. The subtraction of the late follow-up data from the pre-therapy T1-weighted scan demonstrates a decrease in superior pharyngeal constrictor SI (Figure 2c), likely indicating late scarring and fibrosis. A similar effect was observed in the subtraction image between the pre-therapy and early follow-up T2-weighted scans; an early increase was seen in superior pharyngeal constrictor T2 SI, reflecting edema that developed in the mucosa around the superior pharyngeal constrictor (Figure 2f).

Linear RPA revealed that 62.25 Gy represented a “cutoff” value that was associated with alteration in the normalized T1 SI for the superior pharyngeal constrictor in the last follow-up images (logworth=2.214) with ROC area-under-the-curve (AUC) of 0.707 (95% CI, 0.58–0.84; asymptotic significance, P=0.003, Figure 3a). Table 2a shows that patients in cohort that received mean dose ≥ 62.25 Gy to the superior pharyngeal constrictor were associated with significant drop of T1 SI in the follow up scans (P= 0.007, Figure 3b); The soft palate also had decreases in the T1 normalized SI at late follow-up for mean doses >62.25 Gy; however, no candidate D_{mean} “cutpoint” met statistical significance on RPA. While the first split occurred at a dose of 62.9 Gy, the logworth of 1.27 approximated, but failed to reach, the pre-specified statistical significance for the first split (P=0.053). The normalized T1 SI did not change significantly in early follow-up images of both structures, nor was there a dose-response detectable threshold for early T2 enhancement (P=n.s.).

The normalized T2 SIs, which are detailed in Table 2b, did not demonstrate a dose-response relationship, but all patients had significant increases on early follow-up images for both VOIs, irrespective of the mean dose received (P<0.0001 for both SPC and SP, Table 2b). At last follow-up, the normalized T2 SIs for superior pharyngeal constrictor had returned to pre-therapy levels after the initial post-therapy surge (P=0.8, Table 2c), while for the soft palate, they showed significant recovery compared to early post-treatment scans (0.70±0.2 vs. 0.82±0.2, P<0.0001, Table 2b,c) but did not return to initial baseline levels (P<0.0001, Table 2c).

The mean linear dose-response relationships for T1-weighted MRI SI changes between the baseline and late follow-up images qualitatively show decreases above the 62.25 Gy thresholds derived from the linear RPA for both VOIs (Supp. Figure S2a, b). Below 62.25 Gy, the T1 SI differences were less pronounced. Almost all patients showed increases in T2 SI, regardless of the dose delivered (Supp. Figure S2c, d).

To generate SI alteration estimates as a function of dose, we obtained an RPA-derived SI threshold. Using the aforementioned method, a “threshold” normalized T1 alteration of 0.57 was noted for the superior pharyngeal constrictors (logworth=1.42) and confirmed using *post hoc* analytics as the primary candidate for D_{mean}; no other candidates met the pre-specified criteria. A *post hoc* bivariate assessment confirmed discrimination, with a D_{mean} of

63.8 Gy (95% CI, 61.6–66.0) for the group < 0.57 threshold compared to 56.7 Gy (95% CI, 52.2–61.1) for those above 0.57 (Wilcoxon P=0.005). A confirmatory ROC analysis showed an AUC of 0.72 (95% CI, 0.54–0.88; asymptotic significance P=0.013, Figure 4a).

Using the defined threshold as a response indicator, the probability of T1 SI alteration at the specified level was subjected to non-linear fitting using a sigmoidal fit of the observed data, with binning to allow an incidence estimation of T1 SI alteration in 5-Gy bins (Figure 4b). The derived maximum likelihood 2-parameter sigmoidal fitting of the actual collected data showed acceptable fit quality (observed R^2=0.928). Exploratory incidence-adjusted bootstrapped normal tissue probability estimates were then generated as serial curve fits were performed after 10^4 resampling procedures. The resultant sigmoidal curves were fit independently as a function of the continuous dose in 1-Gy bins (Figure 4). Bootstrapped normal tissue complication probability (NTCP) estimates are presented graphically in Figure 4.

Discussion

Our results show that serial MRI acquisitions enable the identification of both early non-dose-related and late dose-dependent RT-induced changes in swallowing structures after definitive IMRT for NPC. The decrease in late follow-up T1-weighted SI likely demonstrates muscle fibrosis that develops over time in patients who receive higher doses, particularly over 62.25 Gy to the superior pharyngeal constrictor VOI [21, 22]. The increase in early post-RT T2-weighted SI likely represents acute RT-induced edema that subsides over time, as suggested by the lack of difference in T2 SI late follow-up images relative to the baseline [21, 22].

Our data, in agreement with those of Nomayr et al. [21], showed high SI for soft palate and superior pharyngeal constrictor on T2 images in the early follow-up period compared to MRI in the pre-treatment period, indicating an acute inflammatory reaction, with edema. No significant change in T1 images was found on early post-RT follow-up. This finding could be attributed to the injured endothelium, which leads to increased permeability and fluid that leaks into the interstitial tissue; resolution occurs once the endothelium has been repaired. Both the soft palate and superior pharyngeal constrictor are composed of striated muscle covered by mucosa. RT-induced edema commonly occurs in soft tissues such as mucosa; however, it is rare in skeletal muscle, which is relatively radioresistant. [35] Therefore, the edema on MRI is likely in the mucosa overlying the superior pharyngeal constrictor and soft palate.

A study by Manara et al. [36] showed that muscle fibrosis and fatty degeneration after RT can be found on histopathological examination. In addition, Khan et al. suggested that direct radiation effects and delayed fibrinoid necrosis of the microvasculature in the muscle are contributors to the pathogenesis of RT-induced muscle atrophy and fibrosis in rabbit skeletal muscle. [35] Our study showed that the decreases in T1-weighted SI between the late follow-up MRI and the pretreatment MRI in the superior pharyngeal constrictor were associated with a higher mean radiation dose (≥62.25 Gy). The change noted on MRI could be attributed to the fibrosis of the skeletal muscle or the mucosa of the superior pharyngeal

constrictor [21, 22]. Since no significant change was noted in the structures receiving <62.25 Gy, it could be a dose threshold that results in fibrosis and subsequent late-onset dysphagia. The threshold of 62.25 Gy found in our study correlates with the findings of a study by Awan et al [20], in which 62.1 Gy delivered to the superior pharyngeal constrictor was a dichotomization point for late RAD due to cranial neuropathies in oropharyngeal cancer patients.

Popovtzer *et al.* demonstrated MRI-detectable anatomical changes in pharyngeal constrictors before and 3 months after chemotherapy and RT of the head and neck in 12 patients. [22] The irradiated constrictors showed increases in T2-weighted MRI SI, irrespective of dose. When the pharyngeal constrictors were stratified on the basis of the mean dose received, those above 50 Gy still had T2 SI increases, with no changes for those receiving less than this value. However, the constrictors receiving >50 Gy showed early decreases in T1 SI changes. The authors suggested that these early changes were correlated to the late dysfunction of the swallowing muscles. Nevertheless, these potentially "dysphagia-predictive" early T1 changes did not manifest in our studied cohort until after further prolonged follow-up, likely due to the chronic nature of the fibrotic process.

Our results are limited by the retrospective nature of this study, including variable MRI acquisition protocols. In addition, we were not able to examine all desired candidate swallowing-related muscles for SI alteration because of the variable extent of the field of view in different patients' scans. Furthermore, although we attempted to extract data regarding dysphagia, the retrospective nature of the dataset precluded an analysis of granular dysphagia endpoints.

Nonetheless, these data demonstrate that RT dose-dependent alteration in functionally important muscle groups can be observed at late time points (>1 year) and suggest that late T1 SI changes from the baseline in superior pharyngeal constrictor can serve as a quantitative imaging biomarker of the previous RT dose. This, along with other patient, disease, and treatment parameters could be incorporated in normal tissue control probability (NTCP) models in attempt to improve the prediction of early and late toxicities and provide tools for radiation plan optimization and early intervention[37–40]

While we sought to implement robust statistical methods (e.g., non-parametric comparison, RPA, and bootstrap resampling techniques), independent confirmation in additional datasets is needed to confirm the veracity of our estimates before large-scale clinical implementation. Our preliminary results were considered hypothesis-generating findings for a prospective study that is currently underway to validate the utility of T1 and T2 SI changes for the prediction of RAD; that study uses patient-reported dysphagia questionnaires and changes seen on modified barium swallow studies (the gold standard) as objective correlates. With further studies, MRI could be used as a tool to evaluate patients after RT and select those at risk for chronic or late-RAD. Ideally, a predictive pattern would be ascertained in which patients are treated more aggressively with earlier dysphagia therapies if MRI biomarkers indicate that they are at high risk for late RAD. In a prospective series, we seek to determine whether T1 SI alterations can be linked with subjective or objective measures of dysphagia or muscle dysfunction.

In conclusion, serial MRI acquisitions enable the identification of both early and late radiation-induced changes in swallowing structures after definitive IMRT for NPC. Dose-dependent T1 SI alterations were observed in the superior pharyngeal constrictors on late scans, suggesting that quantitative dose-response relationships can be observed in the swallowing musculature, most notably at doses in the therapeutic range (i.e., >62.25 Gy). Further efforts will seek to elucidate the relationship between dose-dependent muscle SI changes and the potential functional alteration of swallowing muscles.

Supplementary Material

Refer to Web version on PubMed Central for supplementary material.

Acknowledgments

Funding sources: Dr. Fuller received/receives grant support from the National Institutes of Health/National Cancer Institute Paul Calabresi Clinical Oncology Award Program (K12 CA088084-06) and Clinician Scientist Loan Repayment Program (L30 CA136381-02); the SWOG Hope Foundation Dr. Charles A. Coltman, Jr. Fellowship in Clinical Trials; Elekta AB/MD Anderson Consortium Seed Grant; GE Medical Systems/MD Anderson Center for Advanced Biomedical Imaging In-Kind Award; the MD Anderson Center for Radiation Oncology Research Seed Grant; and the MD Anderson Institutional Research Grant Program Award. Dr. Mohamed received support via the Union for International Cancer Control American Cancer Society International Fellowships for Beginning Investigators. These listed funders/supporters played no role in the study design, collection, analysis, interpretation of data, manuscript writing, or decision to submit the report for publication.

Special thanks to Ann Sutton in scientific publications department whose assistance with editing was helpful in execution of this manuscript.

References

1. Langendijk JA, Doornaert P, Verdonck-de Leeuw IM, Leemans CR, Aaronson NK, Slotman BJ. Impact of late treatment-related toxicity on quality of life among patients with head and neck cancer treated with radiotherapy. Journal of clinical oncology : official journal of the American Society of Clinical Oncology. 2008; 26:3770–6. [PubMed: 18669465]
2. Levendag PC, Teguh DN, Voet P, van der Est H, Noever I, de Kruijf WJM, et al. Dysphagia disorders in patients with cancer of the oropharynx are significantly affected by the radiation therapy dose to the superior and middle constrictor muscle: A dose-effect relationship. Radiother Oncol. 2007; 85:64–73. [PubMed: 17714815]
3. Caudell JJ, Schaner PE, Meredith RF, Locher JL, Nabell LM, Carroll WR, et al. Factors associated with long-term dysphagia after definitive radiotherapy for locally advanced head-and-neck cancer. International journal of radiation oncology, biology, physics. 2009; 73:410–5.
4. Nguyen NP, Moltz CC, Frank C, Vos P, Smith HJ, Karlsson U, et al. Dysphagia following chemoradiation for locally advanced head and neck cancer. Ann Oncol. 2004; 15:383–8. [PubMed: 14998839]
5. Langendijk JA, Doornaert P, Verdonck-de Leeuw IM, Leemans CR, Aaronson NK, Slotman BJ. Impact of late treatment-related toxicity on quality of life among patients with head and neck cancer treated with radiotherapy. Journal of Clinical Oncology. 2008; 26:3770–6. [PubMed: 18669465]
6. Rosenthal DI, Lewin JS, Eisbruch A. Prevention and treatment of dysphagia and aspiration after chemoradiation for head and neck cancer. J Clin Oncol. 2006; 24:2636–43. [PubMed: 16763277]
7. Hughes PJ, Scott PM, Kew J, Cheung DM, Leung SF, Ahuja AT, et al. Dysphagia in treated nasopharyngeal cancer. Head Neck. 2000; 22:393–7. [PubMed: 10862024]
8. Al-Sarraf M, LeBlanc M, Giri PG, Fu KK, Cooper J, Vuong T, et al. Chemoradiotherapy versus radiotherapy in patients with advanced nasopharyngeal cancer: phase III randomized Intergroup study 0099. Journal of clinical oncology : official journal of the American Society of Clinical Oncology. 1998; 16:1310–7. [PubMed: 9552031]

9. Lin JC, Jan JS, Hsu CY, Liang WM, Jiang RS, Wang WY. Phase III study of concurrent chemoradiotherapy versus radiotherapy alone for advanced nasopharyngeal carcinoma: positive effect on overall and progression-free survival. Journal of clinical oncology : official journal of the American Society of Clinical Oncology. 2003; 21:631–7. [PubMed: 12586799]
10. Teguh DN, Levendag PC, Noever I, van Rooij P, Voet P, van der Est H, et al. Treatment techniques and site considerations regarding dysphagia-related quality of life in cancer of the oropharynx and nasopharynx. Int J Radiat Oncol Biol Phys. 2008; 72:1119–27. [PubMed: 18472364]
11. Fua TF, Corry J, Milner AD, Cramb J, Walsham SF, Peters LJ. Intensity-modulated radiotherapy for nasopharyngeal carcinoma: clinical correlation of dose to the pharyngo-esophageal axis and dysphagia. Int J Radiat Oncol Biol Phys. 2007; 67:976–81. [PubMed: 17234360]
12. Lovell SJ, Wong HB, Loh KS, Ngo RY, Wilson JA. Impact of dysphagia on quality-of-life in nasopharyngeal carcinoma. Head Neck. 2005; 27:864–72. [PubMed: 16114007]
13. Chang YC, Chen SY, Lui LT, Wang TG, Wang TC, Hsiao TY, et al. Dysphagia in patients with nasopharyngeal cancer after radiation therapy: a videofluoroscopic swallowing study. Dysphagia. 2003; 18:135–43. [PubMed: 12825907]
14. Wu CH, Hsiao TY, Ko JY, Hsu MM. Dysphagia after radiotherapy: endoscopic examination of swallowing in patients with nasopharyngeal carcinoma. The Annals of otology, rhinology, and laryngology. 2000; 109:320–5.
15. Feng FY, Kim HM, Lyden TH, Haxer MJ, Feng M, Worden FP, et al. Intensity-modulated radiotherapy of head and neck cancer aiming to reduce dysphagia: early dose-effect relationships for the swallowing structures. International journal of radiation oncology, biology, physics. 2007; 68:1289–98.
16. Levendag PC, Teguh DN, Voet P, van der Est H, Noever I, de Kruijf WJ, et al. Dysphagia disorders in patients with cancer of the oropharynx are significantly affected by the radiation therapy dose to the superior and middle constrictor muscle: a dose-effect relationship. Radiother Oncol. 2007; 85:64–73. [PubMed: 17714815]
17. Schwartz DL, Hutcheson K, Barringer D, Tucker SL, Kies M, Holsinger FC, et al. Candidate dosimetric predictors of long-term swallowing dysfunction after oropharyngeal intensity-modulated radiotherapy. International journal of radiation oncology, biology, physics. 2010; 78:1356–65.
18. Kieser JA, Farland MG, Jack H, Farella M, Wang Y, Rohrle O. The role of oral soft tissues in swallowing function: what can tongue pressure tell us? Aust Dent J. 2014; 59:155–61. [PubMed: 24152133]
19. Kumar R, Madanikia S, Starmer H, Yang W, Murano E, Alcorn S, et al. Radiation dose to the floor of mouth muscles predicts swallowing complications following chemoradiation in oropharyngeal squamous cell carcinoma. Oral oncology. 2014; 50:65–70. [PubMed: 24238851]
20. Awan MJ, Mohamed AS, Lewin JS, Baron CA, Gunn GB, Rosenthal DI, et al. Late radiation-associated dysphagia (late-RAD) with lower cranial neuropathy after oropharyngeal radiotherapy: a preliminary dosimetric comparison. Oral Oncol. 2014; 50:746–52. [PubMed: 24906528]
21. Nomayr A, Lell M, Sweeney R, Bautz W, Lukas P. MRI appearance of radiation-induced changes of normal cervical tissues. European radiology. 2001; 11:1807–17. [PubMed: 11511906]
22. Popovtzer A, Cao Y, Feng FY, Eisbruch A. Anatomical changes in the pharyngeal constrictors after chemo-irradiation of head and neck cancer and their dose-effect relationships: MRI-based study. Radiother Oncol. 2009; 93:510–5. [PubMed: 19520446]
23. Ng SH, Liu HM, Ko SF, Hao SP, Chong VF. Posttreatment imaging of the nasopharynx. Eur J Radiol. 2002; 44:82–95. [PubMed: 12413677]
24. Hutcheson KA, Lewin JS, Barringer DA, Lisec A, Gunn GB, Moore MW, et al. Late dysphagia after radiotherapy-based treatment of head and neck cancer. Cancer. 2012; 118:5793–9. [PubMed: 23640737]
25. Takiar V, Ma D, Garden AS, Li J, Rosenthal DI, Beadle BM, et al. Disease control and toxicity outcomes for T4 carcinoma of the nasopharynx treated with intensity modulated radiotherapy. Head Neck. 2015

26. Mohamed AS, Ruangskul MN, Awan MJ, Baron CA, Kalpathy-Cramer J, Castillo R, et al. Quality assurance assessment of diagnostic and radiation therapy-simulation CT image registration for head and neck radiation therapy: anatomic region of interest-based comparison of rigid and deformable algorithms. Radiology. 2015; 274:752–63. [PubMed: 25380454]
27. Walker GV, Awan M, Tao R, Koay EJ, Boehling NS, Grant JD, et al. Prospective randomized double-blind study of atlas-based organ-at-risk autosegmentation-assisted radiation planning in head and neck cancer. Radiother Oncol. 2014; 112:321–5. [PubMed: 25216572]
28. Kocak-Uzel E, Gunn GB, Colen RR, Kantor ME, Mohamed AS, Schoultz-Henley S, et al. Beam path toxicity in candidate organs-at-risk: assessment of radiation emetogenesis for patients receiving head and neck intensity modulated radiotherapy. Radiother Oncol. 2014; 111:281–8. [PubMed: 24746582]
29. Breiman, L. Classification and regression trees. Belmont, Calif: Wadsworth International Group; 1984.
30. Gaspar L, Scott C, Rotman M, Asbell S, Phillips T, Wasserman T, et al. Recursive partitioning analysis (RPA) of prognostic factors in three Radiation Therapy Oncology Group (RTOG) brain metastases trials. International journal of radiation oncology, biology, physics. 1997; 37:745–51.
31. Loh WY. Fifty Years of Classification and Regression Trees. Int Stat Rev. 2014; 82:329–48.
32. Strobl C, Malley J, Tutz G. An Introduction to Recursive Partitioning: Rationale, Application, and Characteristics of Classification and Regression Trees, Bagging, and Random Forests. Psychol Methods. 2009; 14:323–48. [PubMed: 19968396]
33. Efron B. 1977 Rietz Lecture - Bootstrap Methods - Another Look at the Jackknife. Ann Stat. 1979; 7:1–26.
34. Wedenberg M. Assessing the uncertainty in QUANTEC's dose-response relation of lung and spinal cord with a bootstrap analysis. Int J Radiat Oncol Biol Phys. 2013; 87:795–801. [PubMed: 23953634]
35. Khan MY. Radiation-induced changes in skeletal muscle. An electron microscopic study. J Neuropathol Exp Neurol. 1974; 33:42–57. [PubMed: 4812324]
36. Manara G, Mira E. [Histological changes of the human larynx irradiated with various technical therapeutic methods]. Arch Ital Otol Rinol Laringol Patol Cervicofacc. 1968; 79:596–635. [PubMed: 4387753]
37. Brouwer CL, Steenbakkers RJ, Gort E, Kamphuis ME, van der Laan HP, Van't Veld AA, et al. Differences in delineation guidelines for head and neck cancer result in inconsistent reported dose and corresponding NTCP. Radiother Oncol. 2014; 111:148–52. [PubMed: 24560759]
38. Wopken K, Bijl HP, van der Schaaf A, van der Laan HP, Chouvalova O, Steenbakkers RJ, et al. Development of a multivariable normal tissue complication probability (NTCP) model for tube feeding dependence after curative radiotherapy/chemo-radiotherapy in head and neck cancer. Radiother Oncol. 2014; 113:95–101. [PubMed: 25443500]
39. Kierkels RGJ, Korevaar EW, Steenbakkers RJHM, Janssen T, van't Veld AA, Langendijk JA, et al. Direct use of multivariable normal tissue complication probability models in treatment plan optimisation for individualised head and neck cancer radiotherapy produces clinically acceptable treatment plans. Radiother Oncol. 2014; 112:430–6. [PubMed: 25220369]
40. Christianen MEMC, Schilstra C, Beetz I, Muijs CT, Chouvalova O, Burlage FR, et al. Predictive modelling for swallowing dysfunction after primary (chemo)radiation: Results of a prospective observational study. Radiother Oncol. 2012; 105:107–14. [PubMed: 21907437]

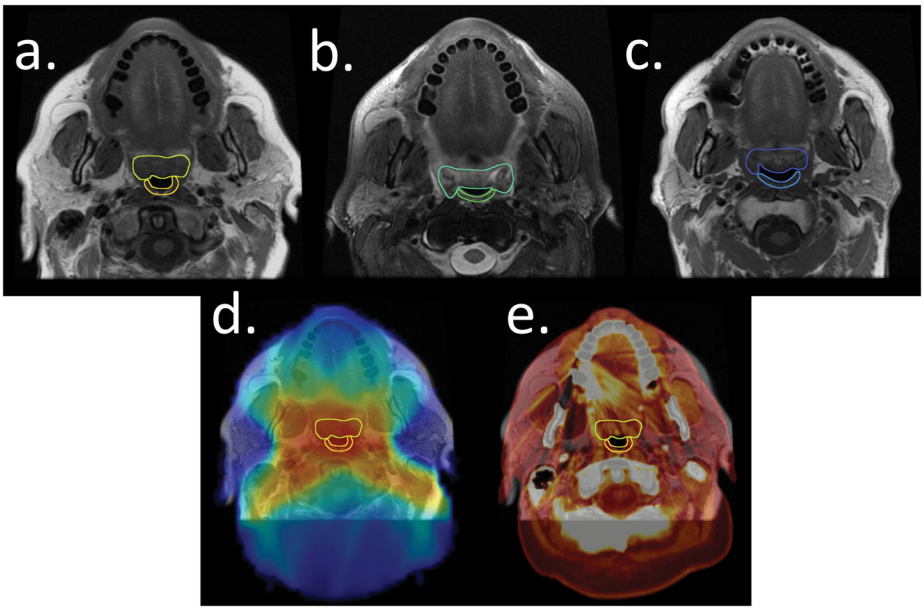

Figure 1.

An example patient illustrates the segmentation of the soft palate (anterior) and the superior pharyngeal constrictor (posterior) and co-registration process. 1a) Patient T1-weighted image at baseline, 1b) T2-weighted image at 3 months after RT, 1c) T1-weighted image at 29 months after RT. 1d) The radiation dose grid superimposed on the T1-weighted MR image. 1e) Co-registration of MRI and planning computed tomography (thermal).

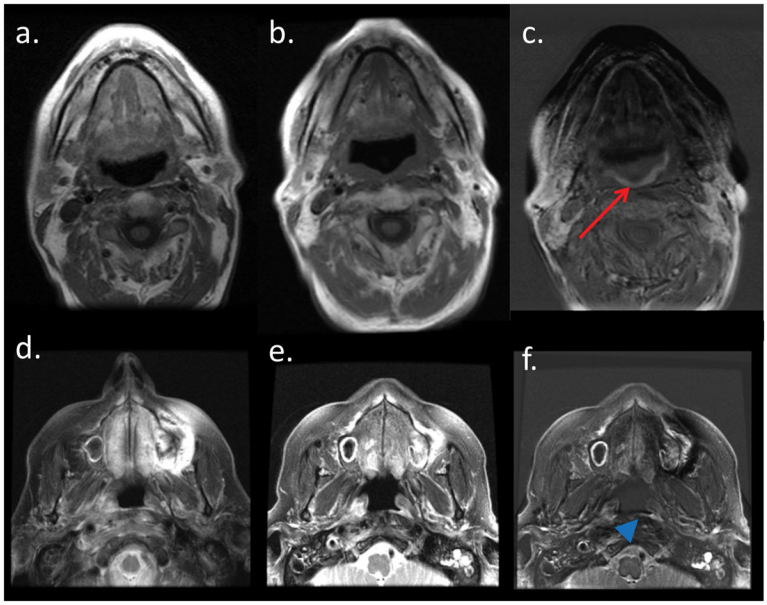

Figure 2.

A subtraction image between the pre-RT T1-weighted MRI (2a) and the late follow-up T1-weighted MRI (2b) shows the outline of the superior pharyngeal constrictor (2c, red arrow), demonstrating the fibrosis that developed between the 2 time points. Another subtraction image between the pre-RT T2-weighted MRI (2d) and the early follow-up T2-weighted MRI (2e) shows the outline of the superior pharyngeal constrictor (2f, blue arrow head), demonstrating the edema that developed between the 2 time points.

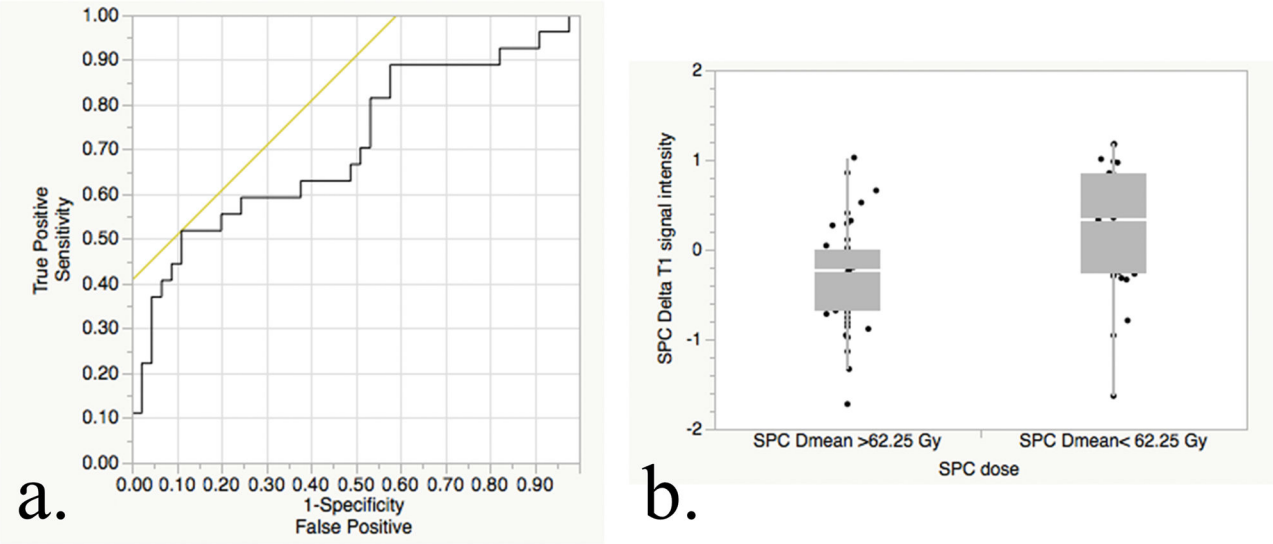

Figure 3.

Dichotomous dose-response assessment. 3a: Confirmatory analysis of the RPA-derived dose-threshold; ROC shows split performance for late T1 SI changes in superior pharyngeal constrictors above and below 62.25 Gy as an AUC of 0.707 (P=0.003, with H_0 denoting AUC =0.5). 3b: Bivariate confirmatory analysis shows distributional plots of T1 SI alteration for superior pharyngeal constrictors, stratified by doses above and below 62.25 Gy.

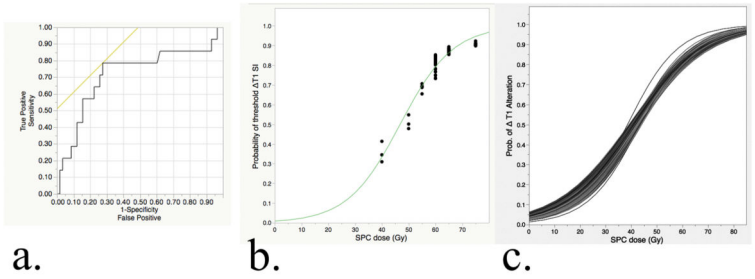

Figure 4.

Continuous (non-linear) dose-response characterization of late T1 superior pharyngeal constrictor SI alteration from the baseline. 4a) Confirmatory analysis of the RPA-derived T1 SI change threshold; ROC shows split performance for T1 SI changes of > or <0.57 in the superior pharyngeal constrictors, as a function of D_{mean}, with an AUC of 0.72 (P=0.013, with H_0 denoting AUC =0.5). 4b) Sigmoidal fit of the observed probability of threshold T1 SI alteration as function of D_{mean} to superior pharyngeal constrictor muscles (R2=0.93). 4c) Incidence-resampled bootstrap predicted the probability of threshold T1 alteration as a function of dose; 10^4 independently resampled distributions were individually fit using a maximum likelihood 2P-sigmoidal function, representing the range of possible dose-response normal tissue complication probability curves to best approximate a “true population incidence.”

Table 1

Table displays patient demographics (age, sex, and ethnicity) for the 72 patients that were completely analyzed. Tumor characteristics included TNM stage and WHO grade. Treatment statistics are shown for RT and chemotherapy. Other induction chemotherapy regimens included combinations of cisplatin, carboplatin, docetaxel, cetuximab, 5-fluorouracil, etoposide, and paclitaxel. Other concurrent chemotherapy regimens included combinations of cisplatin, carboplatin, docetaxel, etoposide, cetuximab, paclitaxel, and erlotinib, unique to certain patients.

Characteristic	Result
Number of patients	72
Median age at RT completion (SD, range)	52 (12, 20–77)
Sex, n (%)	
Female	15 (21%)
Male	57 (79%)
Ethnicity, n (%)	
Asian	10 (14%)
Arabic	2 (3%)
Black	11 (15%)
Caucasian	38 (53%)
Hispanic	10 (14%)
Unknown	1 (1%)
TNM stage, n (%)	
T1	16 (22%)
T2	13 (18%)
T3	12 (17%)
T4	27 (37%)
TX	4 (6%)
N0	11 (15%)
N1	17 (24%)
N2	31 (43%)
N3	8 (11%)
NX	5 (7%)
M0	67 (93%)
M1	5 (7%)
WHO grade, n (%)	
1	7 (10%)
2	26 (36%)
2 to 3	6 (8%)
3	30 (42%)
Unknown	3 (4%)
Dose (Gy), n (%)	
60	2 (3%)
66	4 (5%)

Characteristic	Result
70	66 (91%)
74	1 (1%)
Fractions, n (%)	
30	2 (3%)
32	1 (1%)
33	61 (85 %)
35	8 (11%)
IMRT, n (%)	72 (100%)
Induction chemotherapy, n (%)	
Yes	49 (68%)
No	23 (32%)
Type, n (%)	
TPF	14 (28%)
Cisplatin/docetaxel	10 (20%)
Carboplatin/docetaxel	6 (12%)
Carboplatin/paclitaxel	5 (10%)
TIC	4 (8%)
Modified TPF	3 (6%)
Other	7 (14%)
Concurrent chemotherapy, n (%)	
Yes	63 (87%)
No	9 (13%)
Type, n (%)	
Cisplatin	38 (60%)
Carboplatin	16 (25%)
Cisplatin/carboplatin	3 (5%)
Other	6 (10%)

TPF, docetaxel, cisplatin, fluorouracil; TIC, paclitaxel, ifosfamide, carboplatin.

Table 2

2a) Normalized T1 SI changes between baseline and late follow-up. 2b) Normalized T2 SI changes between baseline and early after RT. 2c) Normalized T2 SI changes between pre-RT and late follow up after RT show a return to baseline for the superior pharyngeal constrictor and a partial recovery for the soft palate. There is a statistically significant decrease in T2 SI between early post-RT and late post-RT for the soft palate (0.82 ± 0.2 vs. 0.70±0.2, P<0.0001) *indicates statistical significance (p <0.05)

a.

		Normalized T1 intensity: mean ± SD		
VOI (#)	**Average mean dose**	**Pre-RT**	**Late Post-RT**	***p***
Superior Pharyngeal Constrictor				
All (72)	62.4 ± 8.7	1.5 ± 0.4	1.4 ± 0.6	0.1
Mean dose <62.25 Gy (25)	53.1 ± 8.4	1.3 ± 0.4	1.6 ± 0.9	0.2
Mean dose ≥ 62.25 Gy (47)	67.3 ± 3.1	1.6 ± 0.4	1.3 ± 0.4	0.007*
Soft Palate				
All (72)	66.8 ± 7.3	1.7 ± 0.5	1.7 ± 0.7	0.3
Mean dose <62.25 Gy (11)	52.8 ± 9.3	1.5 ± 0.3	2.2 ± 1.0	0.2
Mean dose ≥ 62.25 Gy (61)	69.3 ± 2.6	1.7 ± 0.5	1.6 ± 0.5	0.09

b.

		Normalized T2 intensity: mean ± SD		
VOI (#)	**Average mean dose**	**Pre-RT**	**Early Post-RT**	***p***
Superior Pharyngeal Constrictor				
All (72)	62.4 ± 8.7	0.48 ± 0.1	0.73 ± 0.2	<0.0001*
Mean dose <62.25 Gy (25)	53.1 ± 8.4	0.48 ± 0.2	0.71 ± 0.2	<0.0001*
Mean dose ≥ 62.25 Gy (47)	67.3 ± 3.1	0.48 ± 0.1	0.74 ± 0.2	<0.0001*
Soft Palate				
All (72)	66.8 ± 7.3	0.56 ± 0.1	0.82 ± 0.2	<0.0001*
Mean dose <62.25 Gy (11)	52.8 ± 9.3	0.53 ± 0.2	0.76 ± 0.1	0.0008*
Mean dose ≥ 62.25 Gy (61)	69.3 ± 2.6	0.57 ± 0.1	0.83 ± 0.2	<0.0001*

c.

	Normalized T2 intensity: mean ± SD		
VOI (#)	**Pre-RT**	**Late Post-RT**	***p***
Superior Pharyngeal			
Constrictor (72)	0.48 ± 0.1	0.52±0.2	0.8
Soft Palate (72)	0.56 ± 0.1	0.70±0.2	<0.0001*